FUDMA Journal of Sciences (FJS)
ISSN online: 2616-1370
ISSN print: 2645 - 2944
Vol. 10 No. 23, December, 2026, pp 333 – 349
DOI: https://doi.org/10.33003/fjs-2026-1023-6563

Molecular Docking and ADMET Profiling of *Allium cepa* Phytochemicals against Human Pancreatic α-Amylase and Lysosomal Acid α-Glucosidase in Diabetic Management

***Misbaudeen Abdul-Hammed, Ubeydat Temitope Ismail, Al-amin Adeshina Biliaminu, Muhammad Adesina Sharafuddeen, Fasasi Yusuf Olaniyi, Aishat Ayomide Alabi, Firdaus Toyin Makinde**

Computational/ Biophysical Chemistry Unit, Department of Pure and Applied Chemistry, Ladoke Akintola University of Technology (LAUTECH), Ogbomoso, Oyo State, Nigeria.

*Corresponding authors' email: mabdul-hammed@lautech.edu.ng

Received: 01 Oct. 2026
Accepted: 17 Nov. 2026
Published: 18 Nov. 2026

ABSTRACT

Diabetes mellitus is a major global health challenge, and inhibition of carbohydrate-digesting enzymes is one strategy for controlling postprandial hyperglycaemia in type 2 diabetes. *Allium cepa* (onion) contains diverse phytochemicals, but their predicted enzyme-binding and drug-related properties remain poorly characterised. This study aimed to evaluate the predicted binding affinities and pharmacokinetic properties of selected *Allium cepa* phytochemicals against human pancreatic α-amylase (PDB ID: 1HNY) and lysosomal acid α-glucosidase (GAA; PDB ID: 5NN4), the latter used as a structural representative of the GH31 α-glucosidase family. A total of 181 reported phytochemicals were docked using AutoDock Vina in PyRx, with acarbose and miglitol as reference compounds, after validating the protocol by redocking (RMSD 1.14 and 1.20 Å). Top-ranked compounds were further assessed for ADMET properties (ADMETlab 3.0), drug-likeness and oral bioavailability (SwissADME), and predicted activity spectra (PASS). Daucosterol (−9.7 kcal/mol), quercetin (−8.6 kcal/mol), 2,3-dihydroflavon-3-ol, taxifolin, isorhamnetin: −8.5 kcal/mol scored better than acarbose (−6.5 kcal/mol) against α-amylase, while daucosterol (−8.2 kcal/mol) and quercetin (−7.9 kcal/mol) scored better than acarbose (−6.9 kcal/mol) against GAA. Hits interacted with catalytic-site residues, including Asp197, Glu233 and Asp300 of α-amylase. Most hits satisfied Lipinski's rule with no more than one violation and showed acceptable predicted ADMET profiles, although daucosterol is large and poorly soluble. These are computational predictions only; molecular dynamics, in vitro enzyme assays, and testing against intestinal α-glucosidases (maltase-glucoamylase and sucrase-isomaltase) are recommended.

Keywords: *Allium cepa*, A-Amylase, Lysosomal Acid A-Glucosidase, Molecular Docking, ADMET, In Silico Screening.

INTRODUCTION

Diabetes mellitus (DM) is a non-communicable metabolic disorder arising from inadequate insulin production or impaired insulin action, resulting in chronic hyperglycaemia (Ahmed *et al*., 2020; Deshmukh & Jain, 2015). An estimated 537 million adults aged 20–79 years, about 10.5% of the global population, were living with diabetes, and nearly half of all affected adults were unaware of their condition (Hossain *et al*., 2024). Although Africa has the lowest regional prevalence (4.5%), it is projected to experience the steepest rise, about 129% by 2045, to roughly 55 million cases (Hossain *et al*., 2024). Type 2 diabetes (T2D), characterised by insulin resistance, accounts for approximately 90% of cases and is associated with genetic predisposition, obesity and a sedentary lifestyle (Ahmed *et al*., 2020; GBD 2021 Diabetes Collaborators, 2023). Poorly controlled diabetes damages the eyes, kidneys, nerves and cardiovascular system, which increases disability and healthcare costs (Deshmukh & Jain, 2015; Ogunyemi *et al*., 2025).

No definitive cure exists, and management relies on lifestyle modification and pharmacological agents such as metformin, acarbose, miglitol and semaglutide (Ogunyemi *et al*., 2025). One established strategy is to slow carbohydrate digestion and so blunt postprandial glucose peaks. Pancreatic α-amylase hydrolyses the α-1,4 glycosidic bonds of starch (Halim *et al*., 2023), and α-glucosidases then release absorbable glucose from the resulting oligosaccharides (Maulana *et al*., 2022). Acarbose inhibits both enzyme classes, while miglitol acts on α-glucosidases. However, the clinical use of these agents is often limited by gastrointestinal adverse effects, chiefly flatulence, diarrhoea and abdominal pain, which are attributed to the fermentation of undigested carbohydrate in the lower bowel and can reduce adherence (Hedrington & Davis, 2019). These limitations support the search for new, safe and affordable inhibitors from natural sources (Ogunyemi *et al*., 2025).

The α-glucosidases that govern postprandial glucose are the brush-border enzymes maltase-glucoamylase (MGAM) and sucrase-isomaltase (SI), which catalyse the final glucose-releasing steps of starch digestion at the surface of the small intestine (Sim *et al*., 2008, 2010). Human lysosomal acid α-glucosidase (GAA) is a distinct enzyme: it degrades glycogen within lysosomes, and its deficiency causes Pompe disease (Roig-Zamboni *et al*., 2017). Nevertheless, GAA, MGAM and SI all belong to glycoside hydrolase family 31 and have a similar overall architecture (Roig-Zamboni *et al*., 2017; Sim *et al*., 2008). GAA was selected here because a high-resolution crystal structure of the human enzyme (1.83 Å; PDB ID: 5NN4) is available, and it was used as a structural representative of this α-glucosidase family rather than as a therapeutic target in itself. Inhibition of GAA is not a treatment goal and could be an off-target concern. Any

promising compounds must therefore ultimately be evaluated against the intestinal enzymes.

For centuries, medicinal plants have been integral to traditional medical systems worldwide for the treatment of diverse ailments (Ogunyemi *et al.*, 2025; Vivek-Ananth *et al.*, 2023; Zainab *et al.*, 2020). Phytochemicals, the bioactive compounds responsible for the therapeutic properties of these plants form the foundation of many traditional remedies (Vivek-Ananth *et al.*, 2023). Their pharmacological potential makes them invaluable resources in the search for novel drug candidates (Ogunyemi *et al.*, 2025; Abdul-Hammed *et al.*, 2021).

Among these, the onion (*Allium cepa*) stands out as one of the most ancient and widely cultivated vegetables, valued globally for both its culinary and medicinal uses. It is a rich source of phytochemicals such as phenolics, flavonoids, saponins, anthocyanins, organosulfur compounds, quercetin, glycosides, and cysteine sulfoxides, bioactive constituents largely responsible for its therapeutic effects (Durmaz *et al.*, 2023). These compounds exhibit diverse biological activities, including antioxidant, anti-proliferative, anti-inflammatory, and cardioprotective properties, contributing to lipid metabolism regulation, improved insulin sensitivity, and inhibition of key metabolic enzymes associated with metabolic syndrome (Stoica *et al.*, 2021).

Computational approaches such as molecular docking and ADMET profiling reduce the cost, time and resources needed to prioritise candidates before laboratory work (Ibironke *et al*., 2024). Previous work on *Allium cepa* has mostly examined extracts, peel fractions or individual compounds (Drioiche *et al*., 2026; Durmaz *et al*., 2023). A systematic structure-based screening of a broad library of reported *Allium cepa* constituents against these digestive enzymes, combined with pharmacokinetic and drug-likeness profiling, has received less attention. This study aimed to evaluate the predicted binding affinities and pharmacokinetic properties of selected *Allium cepa* phytochemicals against human pancreatic α-amylase and lysosomal acid α-glucosidase using computational methods.

MATERIALS AND METHODS

Compound Library and Reference Inhibitors

A library of 181 isolated phytochemicals reported from *Allium cepa* was compiled from the published literature on its constituents. The compounds were grouped by chemical class, including terpenoids, fatty acyls, flavonoids, phenylpropanoids, benzenoids, organosulfur compounds, steroids, alkaloids and polyketides. Acarbose and miglitol were used as reference compounds. Acarbose is a clinically used inhibitor of both pancreatic α-amylase and intestinal α-glucosidases, and miglitol is a clinically used intestinal α-glucosidase inhibitor. Miglitol is not an established α-amylase inhibitor, so for α-amylase it serves only as a comparator. Two-dimensional or three-dimensional structures of all compounds were downloaded from the PubChem database (https://pubchem.ncbi.nlm.nih.gov/).

Ligand Preparation

Structures were converted to three-dimensional conformers and geometry-optimised in Spartan 14. They were then imported into PyRx (Dallakyan & Olson, 2015), where they were energy-minimised using the Open Babel module with the default universal force field (UFF) and converted to PDBQT format. Protonation states were those assigned by default during PDBQT conversion, and no separate pH-dependent protonation procedure was applied (Bello et al., 2025; Ibironke *et al*., 2024; Ogunyemi *et al*., 2025).

Target Selection and Preparation

Two human enzymes were selected. Pancreatic α-amylase (PDB ID: 1HNY; 1.80 Å) catalyses the first step of starch hydrolysis in the gut lumen. Lysosomal acid α-glucosidase (GAA; PDB ID: 5NN4; 1.83 Å) was used as a structural representative of the glycoside hydrolase family 31 α-glucosidases, which also includes the intestinal enzymes maltase-glucoamylase and sucrase-isomaltase (Roig-Zamboni *et al*., 2017; Sim *et al*., 2008). GAA itself is not the enzyme that controls postprandial glucose absorption, and it is used here as a surrogate. Crystal structures were retrieved from the RCSB Protein Data Bank (http://www.rcsb.org/pdb). In BIOVIA Discovery Studio, water molecules and non-essential heteroatoms were removed, polar hydrogens were added, and the receptor geometry was refined. Prepared receptors were converted to PDBQT format in PyRx (Ogunyemi *et al*., 2025; Ibironke *et al*., 2024; Shoily *et al*., 2025).

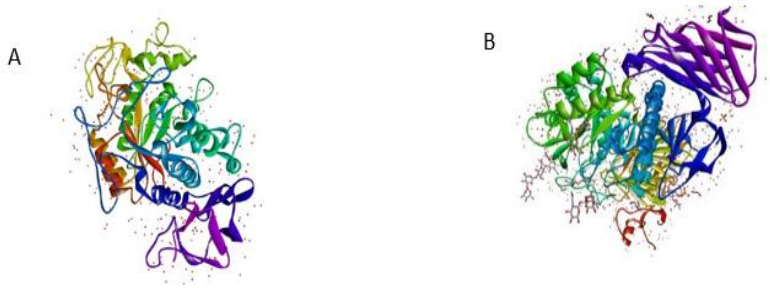


Figure 1: The Crystal Structure of (A) Human Pancreatic Alpha-Amylase (PDB ID: 1HNY) And (B) Human Lysosomal Acid-Alpha-Glucosidase (GAA) (PDB ID: 5NN4)

Identification of Binding Sites

Binding pockets and interacting residues were identified using the Computed Atlas of Surface Topography of Proteins (CASTp) server (http://sts.bioc.uic.edu/castp; Sharma et al., 2020), supplemented by BIOVIA Discovery Studio and the Site Finder module of the Molecular Operating Environment (MOE). The pockets were checked against residues reported for these enzymes in crystallographic studies (Brayer *et al*., 1995; Roig-Zamboni *et al*., 2017). For α-amylase, the catalytic residues are Asp197, Glu233 and Asp300.

Molecular Docking and Protocol Validation

Docking was performed with AutoDock Vina (Trott & Olson, 2010) in PyRx. For each enzyme, the grid box was centred on the identified active-site pocket and sized to enclose it (centre coordinates and dimensions in Table S2). Vina's default

search parameters were used, and the lowest-energy pose of each ligand was retained for analysis. The protocol was validated by cognate redocking: the co-crystallised ligand was extracted, prepared as above and redocked into the same grid. The redocked poses reproduced the crystallographic binding modes with heavy-atom RMSD values of 1.14 Å (1HNY) and 1.20 Å (5NN4), below the accepted 2.0 Å threshold. Interactions (hydrogen bonds, electrostatic, hydrophobic and van der Waals contacts) were visualised in BIOVIA Discovery Studio (Shoily *et al*., 2025; Sunday *et al*., 2025).

Protein–ligand interactions, including hydrogen bonding, hydrophobic interactions, and van der Waals forces, were visualized and analyzed using BIOVIA Discovery Studio (Shoily *et al.,* 2025; Sunday *et al.,* 2025). Docking results were evaluated based on binding affinity (ΔG, kcal/mol) and inhibition constant (Ki). The inhibition constant values were calculated using the binding energy according to Equation (1), which provides a measure of the ligand's potency against its target receptor (Bello *et al.,* 2025).

$$K_i = \exp(\Delta G/RT) \quad (1)$$

$$\text{Ligand Efficiency (LE)} = -(\text{B.E}) \div \text{Heavy atoms (H.A)} \quad (2)$$

$$\text{L.E scale} = 0.873e - 0.026 \times \text{H.A} - 0.064 \quad (3)$$

$$\text{FQ} = \text{LE} \div \text{LEscale} \quad (4)$$

$$\text{LELP} = \text{LogP} \div \text{LE} \quad (5)$$

Where R = Gas constant (1.987×10^{-3} kcal/ mol); T = 298.15K (absolute temperature); K_i = Inhibition Constant and ΔG = Binding energy.

Assessment of Pharmacokinetic Properties and Other Analysis

Pharmacokinetics (PK) describes the dynamic processes governing how a drug is absorbed, distributed, metabolized, and excreted within the body (Sofian *et al.,* 2025). These four processes collectively referred to as ADME, along with toxicity (T), constitute the ADMET profile, which is critical for evaluating the efficacy and safety of potential drug candidates (Fu *et al.,* 2024; Sofian *et al.,* 2025). To reduce the high attrition rate of drug candidates prior to clinical evaluation, advanced *in silico* predictive tools have been developed. In this study, the ADMET properties of the ligands were predicted using the ADMETlab 3.0 web server (https://admetlab3.scbdd.com), an integrated platform for assessing absorption, distribution, metabolism, excretion, toxicity, and physicochemical parameters (Fu *et al.,* 2024; Ogunyemi *et al.,* 2025). The tool facilitated informed decision-making in candidate prioritization during virtual screening.

Furthermore, drug-likeness and oral bioavailability of the phytochemicals and reference drugs were evaluated using the SwissADME web server (http://www.swissadme.ch/) (Bello *et al.,* 2025; Ogunyemi *et al.,* 2025). Lipinski's Rule of Five (RO5) was applied as a benchmark, allowing no more than one violation of the following criteria: molecular weight (MW) ≤ 500 Da, hydrogen bond donors (HBDs) ≤ 5, hydrogen bond acceptors (HBAs) ≤ 10, and partition coefficient (log P) ≤ 5 (Lipinski, 2004).

Prediction of Activity Spectra for Substances (PASS)

The Prediction of Activity Spectra for Substances (PASS) web server (https://www.way2drug.com/passonline/) was employed to predict the potential biological activities of the investigated phytochemicals (Sofian *et al.,* 2025). This computational approach estimates the probability of activity (Pa) and inactivity (Pi) for each compound across a broad range of pharmacological targets, providing valuable insights into their therapeutic potential.

RESULTS AND DISCUSSION

Structural And Active Site Analysis Of The Target Enzymes

Human Pancreatic α-Amylase

The crystal structure of human pancreatic α-amylase (PDB ID: 1HNY; Figure 1A) comprises 496 amino acid residues and contains structural calcium (Ca^{2+}) and chloride (Cl^-) ions. It was solved at 1.80 Å resolution with R-values of 0.174, indicating a high-quality model. α-Amylase hydrolyses the α-1,4 glycosidic bonds of starch and is therefore a target for lowering postprandial glucose (Halim *et al*., 2023). The catalytic residues of the active site are Asp197, Glu233 and Asp300, supported by Arg195, Asn298, Arg337, Asn100, Arg158, Asp167 and His201, which contribute to substrate recognition and to coordination of the Ca^{2+} and Cl^- ions required for stability and activity (Brayer *et al*., 1995).

Human Lysosomal Acid A-Glucosidase (GAA)

The crystal structure of human lysosomal acid α-glucosidase (PDB ID: 5NN4; Figure 1B) was solved at 1.83 Å resolution (R-work 0.154, R-free 0.178). It contains N-acetyl-L-cysteine, triethylene glycol, sulfate, glycerol, 1,2-ethanediol and chloride, which are ligands and crystallisation additives. GAA is a glycoside hydrolase family 31 enzyme that hydrolyses glycosidic bonds in oligosaccharides to release glucose (Maulana *et al*., 2022; Roig-Zamboni *et al*., 2017). Pocket analysis with CASTp and the MOE Site Finder identified residues surrounding the substrate-binding region, including Arg89, Phe90, Asp91, Ala93, Pro94, Asp95, Lys96, Ala97, Ile98, Tyr110, Gly123, Gln124, Pro125, Trp126, Cys127, Trp273, Thr274, Arg275 and Asp319. These residues were used to describe ligand contacts, but they come from pocket analysis and are not all catalytic residues. As stated in the Introduction, GAA is a lysosomal enzyme used here as a structural representative of the GH31 α-glucosidases, and not as the enzyme that controls intestinal glucose absorption.

Molecular Docking Analysis

Molecular docking predicts how a ligand binds to a receptor and estimates the strength of the interaction, which makes it a cost-effective first step in drug discovery (Ibironke *et al*., 2024). Lower binding energy (ΔG) and Ki values indicate stronger predicted binding (Falade *et al*., 2021). All 181 *Allium cepa* phytochemicals and the reference inhibitors were docked against both enzymes. Compounds were then prioritised in stages: docking scores better than acarbose, ADMET profiling, drug-likeness (no more than one Lipinski violation), and ligand efficiency, bioavailability and PASS assessment. Docking results are presented in Tables 1 and 2. Because Vina scores favour larger lipophilic molecules and tend to score polar sugar-mimicking compounds such as acarbose poorly, a better docking score than acarbose indicates stronger predicted binding and does not establish greater inhibitory potency.

Docking Against Human Pancreatic α-Amylase (PDB ID: 1HNY)

Several *Allium cepa* phytochemicals scored better than the reference inhibitors against α-amylase (Table 1). α-Amyrin had the best score (−10.1 kcal/mol; Ki = 0.04 µM), followed by the steroidal saponins alliospiroside-B and alliospiroside-D (−9.9 kcal/mol each), diosgenin (−9.8 kcal/mol), and β-amyrin, cycloartenol and daucosterol (−9.7 kcal/mol each). Among flavonoids, quercetin (−8.6 kcal/mol; Ki = 0.49 µM), 2,3-dihydroflavon-3-ol, isorhamnetin and taxifolin (−8.5 kcal/mol; Ki = 0.58 µM each) were the best. The reference

inhibitors scored lower: acarbose −6.5 kcal/mol (Ki = 17.08 μM) and miglitol −5.5 kcal/mol (Ki = 92.48 μM). These results identify several compounds with higher predicted affinity than the reference inhibitors, but the scores are computational estimates and need experimental confirmation.

Docking Against Human Lysosomal Acid A-Glucosidase (GAA, PDB ID: 5NN4)

Against GAA, β-amyrin had the best score (−9.6 kcal/mol; Ki = 0.09 μM), followed by α-amyrin (−9.5 kcal/mol), the alliospirosides (−9.3 to −9.0 kcal/mol) and oleanolic acid (−9.0 kcal/mol) (Table 2). Daucosterol (−8.2 kcal/mol; Ki = 0.97 μM) and quercetin (−7.9 kcal/mol; Ki = 1.61 μM) were also better than the reference inhibitors, acarbose (−6.9 kcal/mol; Ki = 8.69 μM) and miglitol (−5.1 kcal/mol; Ki = 181.72 μM). Some compounds scored equal to acarbose (for example vanillic acid at −6.9 kcal/mol), and these are not described as stronger binders. Because GAA is a surrogate for the intestinal α-glucosidases, these scores indicate general binding tendencies for the GH31 family and do not show that the compounds inhibit the enzymes that control glucose absorption.

Table 1: Docking Scores and Inhibition Constants of Phytochemicals from *Alium Cepa* and Standard Drugs Against 1hny

S/N	Ligands	Binding Affinity (kcal/mol)	Inhibition Constant, Ki ($_{u}$M)
1	alpha-Amyrin	-10.1	0.04
2	Alliospiroside-B	-9.9	0.05
3	Alliospiroside-D	-9.9	0.05
4	Diosgenin	-9.8	0.06
5	Beta-amyrin	-9.7	0.08
6	Cycloartenol	-9.7	0.08
7	Daucosterol	-9.7	0.08
8	Alliospiroside-A	-9.6	0.09
9	Alliospiroside-C	-9.6	0.09
10	Cycloartanol	-9.5	0.11
11	Oleanolic acid	-9.5	0.11
12	Quercetin-3,4'-diglucoside	-9.2	0.18
13	Cycloeucalenol	-9.1	0.21
14	Alliofuroside	-9.0	0.25
15	Oleanoic acid	-9.0	0.25
16	Rutin	-8.9	0.30
17	Cholesterol	-8.8	0.35
18	24-Methylenecycloartanol	-8.7	0.42
19	Quercetin	-8.6	0.49
20	2,3-Dihydroflavon-3-ol	-8.5	0.58
21	Isorhamnetin	-8.5	0.58
22	Taxifolin	-8.5	0.58
23	Quercetin-3,4'-diglucoside	-8.4	0.70
24	Spiraeoside	-8.4	0.70
25	Kaempferol	-8.3	0.82
26	Quercetin-3-glucoside	-8.2	0.97
27	Heptadecane	-8.1	1.15
28	Isorhamnetin-3-glucoside	-8.1	1.15
29	Zeaxanthin	-7.9	1.16
30	Beta-Tocopherol	-7.7	2.25
31	Isoquercitrin	-7.6	2.67
32	1-O-(4-Coumaroyl)-beta-D-glucose	-7.3	4.42
33	1-O-feruloyl-beta-D-glucose	-7.3	4.42
34	Riboflavin	-7.3	4.42
35	1-Caffeoyl-beta-D-glucose	-7.2	5.24
36	beta-Carotene	-7.1	6.20
37	Melatonin	-7.1	6.20
38	Diallyl-sulfide	-6.9	8.69
39	Cyclopentadecanone	-6.8	10.29
40	Abscisic-acid	-6.7	12.20
41	Caffeic acid	-6.4	20.23
42	ACARBOSE (STANDARD)	-6.5	17.08
43	MIGLITOL (STANDARD)	-5.5	92.48

Table 2: Docking Scores and Inhibition Constants of Phytochemicals from *Allium Cepa* and Standard Drugs Against 5nn4

S/N	Ligands	Binding Affinity (Kcal/mol)	Inhibition Constant, Ki uM)
1	Beta-amyrin	-9.6	0.09
2	Alpha-Amyrin	-9.5	0.11
3	Alliospiroside-A	-9.3	0.15
4	Alliospiroside-D	-9.2	0.18
5	Alliospiroside-B	-9.1	0.21
6	Alliospiroside-C	-9.0	0.25
7	Oleanolic-acid	-9.0	0.25
8	Alliofuroside-A	-8.8	0.35
9	Diosgenin	-8.8	0.35
10	Oleanoic-acid	-8.8	0.35
11	Beta-Carotene	-8.7	0.42
12	Rutin	-8.6	0.49
13	Zeaxanthin	-8.6	0.49
14	Cycloeucalenol	-8.4	0.70
15	Daucosterol	-8.2	0.97
16	Isoquercitrin	-8.2	0.97
17	Spiraeoside	-8.2	0.97
18	24-Methylenecycloartanol	-8.1	1.15
19	Cycloartanol	-8.0	1.36
20	Cycloartenol	-8.0	1.36
21	Quercetin-3,4'-diglucoside	-7.9	1.61
22	Quercetin	-7.9	1.61
23	Heptadecane	-7.7	2.25
24	Riboflavin	-7.7	2.25
25	Cholesterol	-7.5	3.16
26	Quercetin-3-glucoside	-7.5	3.16
27	2,3-Dihydroflavon-3-ol	-7.4	3.74
28	Isorhamnetin-3-glucoside	-7.4	3.74
29	Isorhamnetin	-7.3	4.42
30	Kaempferol	-7.3	4.42
31	Taxifolin	-7.2	5.24
32	Quercetin	-7.0	7.34
33	1-Caffeoyl-beta-D-glucose	-6.9	8.69
34	Vanilic-acid	-6.9	8.69
35	ACARBOSE (STANDARD)	-6.9	8.69
36	MIGLITOL (STANDARD)	-5.1	181.72

ADMET Analysis of the Selected Compounds

Absorption, Distribution, Metabolism, Excretion, and Toxicity (ADMET) evaluation represents a crucial stage in early drug discovery, ensuring that potential therapeutic agents possess both efficacy and favorable pharmacokinetic behavior (Fu *et al.*, 2025). A promising drug candidate must not only exhibit strong activity against its biological target but also display acceptable ADMET characteristics at therapeutic concentrations (Ibironke *et al.*, 2024). Assessing these parameters at the computational stage minimizes the risk of drug failure, as more than 50% of drug candidates are reported to fail due to poor ADMET properties (Fu *et al.*, 2025).

In this study, the ADMET properties of the selected ligands were predicted using the ADMETlab 3.0 web server (https://admetlab3.scbdd.com). Only bioactive compounds that demonstrated higher binding affinities than the standard drugs were subjected to ADMET screening, as presented in Table 3. The interpretative criteria for each endpoint were based primarily on the ADMETlab 3.0 documentation (ADMETlab), supplemented with established benchmarks reported by Manhas *et al.*, (2024) for best practices in ADMET profiling.

For absorption, compounds with Human Intestinal Absorption (HIA) values greater than 30% and Caco-2 permeability values above −5.15 (log unit) were considered to possess good intestinal permeability, indicating an enhanced likelihood of efficient absorption within the gastrointestinal tract (Manhas *et al.*, 2024; Bello *et al.*, 2025). For distribution parameters, Plasma Protein Binding (PPB) ≤ 90% and Blood Brain Barrier (BBB) permeability ($-1 < \log BB < 0.3$) were regarded as optimal ranges. These thresholds reflect a balance between systemic bioavailability and minimal central nervous system penetration (Manhas *et al.*, 2024). Metabolic evaluation focused on the interaction of the compounds with the cytochrome P450 (CYP450) isoenzymes (CYP1A2, CYP2C9, CYP2C19, CYP2D6, and CYP3A4) which play a central role in xenobiotic metabolism. Nearly all the selected phytochemicals were predicted to be non-inhibitors (−) of these CYP450 enzymes, indicating a low risk of metabolic interference or drug–drug interactions (Bello *et al.*, 2025).

Excretory parameters were assessed based on plasma half-life (t½) and plasma clearance (Cl). Compounds with half-life values between 1–4 hours and plasma clearance rates below 15 mL/min/kg were considered to exhibit favorable excretion

profiles, supporting sustained yet non-toxic systemic exposure.

Toxicity endpoints, expressed as probabilistic values, were evaluated within an acceptable range (typically < 0.7). Compounds predicted to be non-mutagenic in the Ames test, non-carcinogenic in the carcinogenicity (C) assessment, non-hepatotoxic in the hepatotoxicity (HP) test, and non-inhibitory toward hERG and OAT transporters were classified as safe candidates. A few compounds displayed mild eye irritation or corrosivity in the eye irritation (EI) and eye corrosion (EC) tests; however, such liabilities can be optimized during the lead refinement stage of drug development (Abdul-Hammed *et al.*, 2021).

Predicted plasma protein binding was high (above 90%) for quercetin (98.66%), isorhamnetin (98.34%), 2,3-dihydroflavon-3-ol (95.82%) and taxifolin (95.11%) and lower for daucosterol (79.68%). For metabolism, daucosterol was not flagged as an inhibitor of any of the five cytochrome P450 isoforms examined (CYP1A2, CYP2C9, CYP2C19, CYP2D6, CYP3A4). Quercetin and isorhamnetin were flagged for CYP1A2 and CYP3A4 (isorhamnetin also for CYP2C9), taxifolin for CYP3A4, and 2,3-dihydroflavon-3-ol for CYP2C19, CYP2C9 and CYP3A4, which raises the possibility of drug–drug interactions. Predicted intestinal absorption varied between compounds, and large glycosides such as alliofuroside (889 Da) were predicted to be poorly absorbed. For inhibitors intended to act in the gut lumen, as acarbose does, limited absorption is not necessarily a disadvantage. The most frequent toxicity flags among the prioritised compounds were eye irritation or corrosion (for example quercetin, taxifolin, isorhamnetin, 2,3-dihydroflavon-3-ol and caffeic acid), while daucosterol was not flagged for these. These flags are typically addressed during later lead optimisation (Abdul-Hammed *et al*., 2021). These endpoints are machine-learning predictions, so they only guide prioritisation and cannot replace experimental ADMET and toxicity testing.

Table 3: ADMET Profiling of the Studied Phytochemicals from *Allium cepa* and the Standards

Compounds	**Absorption and Distribution**				**Metabolism**					**Excretion**		**Toxicity**				
	BBB; (+/-)	HIA	PPB	CaCo-2	2C19	1A2	3A4	2C9	2D6	CL-plasma	HL	EC	HI	C	HP	OAT
beta-Tocopherol;	0.78; (+)	0.00; (-)	94.37; (+)	-5.01; (-)	+	-	+	+	-	5.19; (-)	0.48; (+)	+	0.71; (+)	-	-	-
1-Caffeoyl-beta-D-glucose;	0.01; (-)	0.90; (+)	67.89; (-)	-6.36; (+)	-	-	-	-	-	3.61; (-)	2.65; (-)	-	0.02; (-)	-	+	-
Riboflavin;	0.00; (-)	0.00; (-)	58.31; (-)	-5.53; (+)	-	+	-	-	-	2.80; (-)	1.92; (-)	-	0.04; (-)	-	+	-
Melatonin;	0.01; (-)	0.61; (-)	51.16; (-)	-4.83; (-)	-	+	-	-	-	7.85; (-)	0.84; (+)	-	0.20; (-)	-	+	-
Vanilic acid	0.00; (-)	0.11; (-)	67.70; (-)	-5.10; (-)	-	-	-	-	-	3.04; (-)	1.98; (-)	+	0.04; (-)	-	-	-
Cyclopentadecanone;	0.97; (+)	0.00; (-)	60.62; (-)	-4.94; (-)	-	-	-	-	-	5.78; (-)	0.12; (+)	+	0.25; (-)	-	-	-
Quercetin-3,4'-diglucoside;	0.00; (-)	0.86; (+)	82.65; (-)	-6.80; (+)	-	-	-	-	-	1.84; (-)	5.38; (-)	-	0.00; (-)	-	+	-
Rutin;	0.00; (-)	0.64; (-)	85.00; (-)	-6.55; (+)	-	-	-	-	-	1.61; (-)	4.62; (+)	-	0.01; (-)	-	-	-
Quercetin;	0.00; (-)	0.13; (-)	98.66; (+)	-6.18; (+)	-	+	+	-	-	8.29; (-)	1.59; (-)	-	0.05; (-)	-	-	-
2,3-Dihydroflavon-3-ol;	0.96; (+)	0.01; (-)	95.82; (+)	-4.88; (-)	+	-	+	+	-	5.87; (-)	2.02; (-)	-	0.21; (-)	-	-	-
Isorhamnetin;	0.00; (-)	0.12; (-)	98.34; (+)	-5.48; (+)	-	+	+	+	-	3.86; (-)	1.70; (-)	-	0.06; (-)	-	-	-
Spiraeoside;	0.00; (-)	0.76; (+)	86.47; (-)	-6.33; (+)	-	-	-	-	-	2.85; (-)	3.78; (-)	-	0.01; (-)	-	-	-
kaempferol;	0.00; (-)	0.02; (-)	97.88; (+)	-5.97; (+)	-	+	+	+	-	5.69; (-)	1.39; (-)	-	0.07; (-)	+	-	-
Quercetin-3-glucoside;	0.00; (-)	0.19; (-)	84.36; (-)	-6.26; (+)	-	-	+	-	-	3.53; (-)	3.63; (-)	-	0.01; (-)	-	-	-
Isoquercitrin;	0.00; (-)	0.19; (-)	84.36; (-)	-6.26; (+)	-	-	+	-	-	3.53; (-)	3.63; (-)	-	0.01; (-)	-	-	-
Taxifolin;	0.01; (-)	0.07; (-)	95.11; (+)	-6.15; (+)	-	-	+	-	-	13.38; (+)	2.09; (-)	-	0.06; (-)	-	-	-
Isorhamnetin-3-glucoside;	0.00; (-)	0.20; (-)	84.92; (-)	-6.29; (+)	-	-	-	+	-	2.57; (-)	3.48; (-)	-	0.01; (-)	-	-	-
Diallyl sulfide;	0.16; (-)	0.01; (-)	76.89; (-)	-4.55; (-)	+	+	+	-	+	11.60; (+)	1.09; (-)	+	0.08; (-)	-	-	-
1-O-(4-Coumaroyl)-beta-D-glucose;	0.00; (-)	0.71; (+)	76.72; (-)	-6.25; (-)	-	-	-	-	-	2.94; (-)	2.47; (-)	-	0.03; (-)	-	+	-
1-O-feruloyl-beta-D-glucose;	0.00; (-)	0.90; (-)	69.35; (-)	-6.05; (-)	-	-	-	-	-	2.81; (-)	2.53; (-)	-	0.02; (-)	-	-	-; ;
Caffeic acid;	0.00; (-)	0.30; (-)	64.67; (-)	-4.94; (-)	-	-	-	-	-	14.36; (+)	2.07; (-)	+	0.04; (-)	-	-	-
Alliospiroside B;	0.16; (-)	0.44; (-)	50.41; (-)	-6.14; (+)	-	-	-	-	-	1.43; (-)	3.47; (-)	-	0.15; (-)	-	-	-
Alliospiroside D;	0.08; (-)	0.78; (+)	42.05; (-)	-6.25; (+)	-	-	-	-	-	1.23; (-)	4.09; (-)	-	0.13; (-)	-	-	-
Alliospiroside A;	0.06; (-)	0.12; (-)	51.37; (-)	-6.03; (+)	-	-	-	-	-	1.83; (-)	3.44; (-)	-	0.20; (-)	-	-	-
Alliospiroside C;	0.03; (-)	0.40; (-)	42.89; (-)	-6.10; (+)	-	-	-	-	-	1.66; (-)	4.10; (-)	-	0.17; (-)	-	-	-
Alliofuroside;	0.00; (-)	1.00; (+)	27.10; (-)	-6.66; (+)	-	-	-	-	-	0.32; (-)	4.16; (+)	-	0.12; (-)	-	-	-
Cycloeucalenol;	0.47; (-)	0.00; (-)	96.50; (+)	-4.98; (-)	-	-	-	-	-	13.52; (+)	0.85; (+)	-	0.13; (-)	+	-	-

Compounds	Absorption and Distribution				Metabolism					Excretion			Toxicity			
Cholesterol;	0.35; (-)	0.00 ; (-)	84.81 ; (-)	-5.22; (-)	-	-	-	-	-	13.19; (+)	0.55 ; (+)	-	0.18 ; (-)	+	-	-
alpha-Amyrin;	0.99; (-)	0.00 ; (-)	97.96 ; (-)	-5.51; (-)	-	-	-	+	-	11.00; (-)	0.17 ; (-)	-	0.08 ; (-)	+	-	-
Cycloartenol;	0.51; (-)	0.00 ; (-)	94.64 ; (+)	-4.91; (-)	-	-	-	-	-	17.09; (+)	0.92 ; (+)	-	0.13 ; (-)	+	-	-
Oleanolic acid;	0.64; (-)	0.00 ; (-)	96.48 ; (+)	-5.50; (+)	-	-	-	-	-	4.89; (-)	0.68 ; (-)	-	0.04 ; (-)	+	+	-
Zeaxanthin;	0.00; (-)	0.00 ; (-)	92.48 ; (+)	-5.07; (-)	-	-	-	-	-	9.27; (-)	0.60 ; (+)	-	0.12 ; (-)	+	-	-
beta-Carotene;	0.00; (-)	0.00 ; (-)	94.20 ; (+)	-4.89; (-)	+	-	+	-	-	8.92; (-)	0.24 ; (-)	-	0.15 ; (-)	+	-	-;
Abscisic acid;	0.00; (-)	0.00 ; (-)	47.99 ; (-)	-4.93; (-)	+	-	-	-	-	2.59; (-)	1.46 ; (-)	-	0.03 ; (-)	+	-	-
Oleanoic acid;	0.26; (-)	0.00 ; (-)	91.08 ; (-)	-5.41; (-)	-	-	-	-	-	4.96; (-)	0.88 ; (-)	+	0.03 ; (-)	+	+	-
Diosgenin;	0.25; (-)	0.00 ; (-)	83.81 ; (-)	-5.07; (-)	-	-	-	-	-	17.36; (+)	1.51 ; (-)	-	0.22 ; (-)	+	-	-
Beta-amyrin;	0.99; (+)	0.00 ; (-)	97.79 ; (+)	-5.30; (+)	+	-	-	+	-	10.18; (+)	0.13 ; (-)	-	0.07 ; (-)	+	-	-
Daucosterol;	0.02; (-)	0.00 ; (-)	79.68 ; (-)	-5.38; (-)	-	-	-	-	-	3.88; (-)	1.19 ; (-)	-	0.13 ; (-)	-	-	-
Cycloartanol; ;	0.86; (-)	0.00 ; (-)	88.92 ; (-)	-5.10; (-)	+	-	-	+	+	14.45; (-)	0.55 ; (-)	-	0.13 ; (-)	+	-	-
Acarbose;	1; (+)	nill	1.00; (-)	-6.47; (+)	+	-	-	-	+	0.00; (-)	0.00 ; (+)	-	nill	-	-	+
Miglitol	0.53; (-)	0.00 ; (-)	-8.32; (-)	-5.33; (+)	-	-	-	-	-	6.30; (-)	1.90 ; (-)	+	0.21 ; (-)	-	-	-

Drug Likeness Analysis of the Selected Compounds and Standards

The drug-likeness of the selected phytochemicals was assessed using Lipinski's Rule of Five (RO5), which serves as a fundamental guideline for evaluating the oral bioavailability of drug-like compounds (Lipinski, 2004). According to this rule, an orally active compound should possess a molecular weight (MW) ≤ 500 g/mol, an octanol–water partition coefficient (Log P) ≤ 5, no more than 10 hydrogen bond acceptors (HBA), and a maximum of 5 hydrogen bond donors (HBD). A compound is generally considered drug-like if it violates no more than one of these parameters. As presented in Table 4, several compounds exhibited molecular weights exceeding 500 Da, such as Alliospiroside B (738.90 Da), Alliospiroside A (708.88 Da), Alliofuroside (889.03 Da), Alliospiroside D (754.90 Da), and Daucosterol (576.85 Da). In addition to their elevated molecular weights, these compounds possessed more than 5 HBDs and more than 10 HBAs except for Daucosterol thereby violating Lipinski's criteria and suggesting potential limitations in oral bioavailability.

Moderate to high molecular weight compounds (300–500 Da), such as Taxifolin (304.25 Da), Quercetin (302.24 Da), Isorhamnetin (316.26 Da), and 1-O-Feruloyl-β-D-glucose (356.32 Da), conformed to RO5, indicating favorable predicted drug-like characteristics. Compounds with lower molecular weights (< 300 Da) generally exhibited superior predicted oral bioavailability and drug-likeness. Notable examples include valinic acid, cyclopentadecanone, heptadecane, 2,3-dihydroflavon-3-ol, caffeic acid, and diallyl sulfide. Their relatively small molecular sizes and balanced HBA/HBD profiles highlight their potential as promising pharmacological candidates.

Among the reference standards, all compounds had no more than one violation, except Acarbose. Despite this, they demonstrated excellent drug-like characteristics, although their miLog P values were below 0, indicating greater aqueous solubility compared to lipid solubility. Conversely, smaller molecules with moderate lipophilicity (miLog P = 2–5) including cyclopentadecanone, 2,3-dihydroflavon-3-ol, and diallyl sulfide tend to maintain a favorable balance between solubility and permeability, making them particularly attractive for further drug development (Bello *et al.*, 2025). Compounds exhibiting no more than one violation of Lipinski's criteria were selected for subsequent pharmacokinetic and pharmacodynamic analyses.

Table 4: Drug-Likeness of The Hit Compounds and Standard Drugs

Compounds	Heavy atoms (HA)	Molecular Weight (MW)	RO5 Violations	Hydrogen Bond Donors	Hydrogen Bond Acceptors	miLogP
BENZENOIDS						
Vanilic acid	12	168.15	0	2	4	1.08
FLAVONOIDS						
Taxifolin	22	304.25	0	5	7	0.51
Quercetin	22	302.24	0	5	7	1.23
2,3-Dihydroflavon-3-ol	18	240.25	0	1	3	2.08
Isorhamnetin	23	316.26	0	4	7	1.65
PHENYLPROPANOIDS						
Caffeic acid	13	180.16	0	3	4	0.93
1-O-feruloyl-beta-D-glucose	25	356.32	0	5	9	-0.34
TERPENOIDS						

Compounds	Heavy atoms (HA)	Molecular Weight (MW)	RO5 Violations	Hydrogen Bond Donors	Hydrogen Bond Acceptors	miLogP
Daucosterol	41	576.85	1	4	6	3.96
STEROIDS						
Alliospiroside B	52	738.90	3	7	13	1.07
Alliospiroside A	50	708.88	3	6	12	1.94
Alliofuroside	62	889.03	3	11	18	-0.37
Alliospiroside D	53	754.90	3	8	14	-0.67
ORGANOSULFUR						
Diallyl sulfide	7	114.21	0	0	0	2.14
STANDARDS						
Acarbose	44	645.6	3	14	19	-6.24
Miglitol	14	204.22	0	5	6	-1.94

Bioactivity Test of the Selected Ligands and Standard Drugs

The bioactivity properties of all selected hit compounds and standard drugs were evaluated using the established Equations (2–5) as described by Bello *et al.,* (2025). The inverse relationship between binding energy and inhibition constant (Eq. 1) implies that higher binding affinity corresponds to lower inhibition constants (Ogunyemi *et al.,* 2025). Typically, a promising lead compound exhibits an inhibition constant (Ki) within the range of 0.1–1.0 μM, and not exceeding 10 nM for an ideal drug (Ogunyemi *et al.,* 2025). As shown in Tables 5 and 6, all selected hit compounds demonstrated inhibition constant values ranging from 0.08 to 20.20 μM and 0.97 to 8.69 μM, respectively. These values qualify the compounds as potential hits, with Daucosterol exhibiting the highest inhibitory potency among them. The Ligand Efficiency (LE), Fit Quality (FQ), and Ligand-Efficiency-Dependent Lipophilicity (LELP) were calculated for each compound using Equations (2–5). The recommended threshold values for these parameters are LE ≥ 0.3, FQ ≥ 0.8, and LELP between −10 and 10. The results summarized in Tables 5 and 6 show that nearly all the selected ligands meet these criteria. Specifically, most compounds displayed LE values ≥ 0.3 and FQ values ≥ 0.8, while their LELP values were within the optimal range of −10 to 10, confirming their potential as viable drug candidates (Abdul-Hammed *et al.,* 2021).

The bioactivity profiling of *Allium cepa* phytochemicals against human pancreatic α-amylase (PDB ID: 1HNY) revealed several promising hits with diverse molecular efficiencies and lipophilic properties (Table 5). Daucosterol emerged as the most predicted active compound, exhibiting LE values between 0.2 and 0.3 and an LELP of 14.04, indicating a balance between efficiency and target binding. Other key compounds; Quercetin, 2,3-Dihydroflavon-3-ol, and Taxifolin demonstrated strong activity, with LE values of 0.49, 0.58, and 0.58, respectively, and favorable LELP scores consistent with high ligand efficiency. Additional bioactive compounds such as Heptadecane, Isorhamnetin, 1-O-Feruloyl-β-D-glucose, Diallyl sulfide, Cyclopentadecanone, and Caffeic acid also showed significant inhibitory potential, characterized by acceptable LE (~0.3–0.99) and high heavy atoms (HA) counts, making them strong candidates for further optimization.

Against α-amylase (Table 5), the flavonoids quercetin, 2,3-dihydroflavon-3-ol, taxifolin and isorhamnetin met all three criteria (LE 0.37–0.47, FQ 0.89–0.98, LELP 1.3–4.5), meaning they achieve their predicted affinity efficiently for their size. Daucosterol has the best score among these compounds but a low LE (0.24) and a high LELP (16.74), so its affinity is driven partly by its size and lipophilicity rather than by efficient binding. Diallyl sulfide shows very high efficiency (LE 0.99) only because it has seven heavy atoms, so efficiency values of very small molecules are inflated and should be read with caution. Both reference compounds, particularly acarbose (LE 0.15), had lower efficiency than the flavonoids. Against GAA (Table 6), quercetin and 2,3-dihydroflavon-3-ol had the most favourable profiles, daucosterol was again inefficient (LE 0.20; LELP 19.80), and isorhamnetin and taxifolin had FQ values (0.76) just below the 0.8 guideline.

Table 5: Ligand-Efficiency Metrics Against A-Amylase (1hny)

Ligand	ΔG (kcal/mol)	Ki (μM)	HA	LE	LE scale	FQ	miLogP	LELP
Daucosterol	−9.7	0.08	41	0.24	0.24	1.00	3.96	16.74
Quercetin	−8.6	0.49	22	0.39	0.43	0.91	1.23	3.15
2,3-Dihydroflavon-3-ol	−8.5	0.58	18	0.47	0.48	0.98	2.08	4.40
Taxifolin	−8.5	0.58	22	0.39	0.43	0.90	0.51	1.32
Isorhamnetin	−8.5	0.58	23	0.37	0.42	0.89	1.65	4.46
1-O-Feruloyl-β-D-glucose	−7.3	4.42	25	0.29	0.39	0.75	−0.34	−1.16
Diallyl sulfide	−6.9	8.69	7	0.99	0.66	1.49	2.14	2.17
Cyclopentadecanone	−6.8	10.29	16	0.42	0.51	0.83	4.37	10.28
Caffeic acid	−6.4	20.23	13	0.49	0.56	0.88	0.93	1.89
Acarbose (reference)	−6.5	17.08	44	0.15	0.21	0.69	−6.24	−42.24
Miglitol (reference)	−5.5	92.48	14	0.39	0.54	0.72	−1.94	−4.94

Table 6: Ligand-Efficiency Metrics Against GAA (5NN4)

Ligand	ΔG (kcal/mol)	Ki (μM)	HA	LE	LE scale	FQ	miLogP	LELP
Daucosterol	−8.2	0.97	41	0.20	0.24	0.85	3.96	19.80
Quercetin	−7.9	1.61	22	0.36	0.43	0.84	1.23	3.43
2,3-Dihydroflavon-3-ol	−7.4	3.74	18	0.41	0.48	0.85	2.08	5.06
Isorhamnetin	−7.3	4.42	23	0.32	0.42	0.76	1.65	5.20
Taxifolin	−7.2	5.24	22	0.33	0.43	0.76	0.51	1.56
Vanillic acid	−6.9	8.69	12	0.58	0.58	1.00	1.08	1.88
Acarbose (reference)	−6.9	8.69	44	0.16	0.21	0.73	−6.24	−39.79
Miglitol (reference)	−5.1	181.72	14	0.36	0.54	0.67	−1.94	−5.33

Oral Bioavailability Analysis of the Selected Ligands and Standards

Hit compounds exhibiting favorable predicted ADMET and drug-likeness profiles were further evaluated for their oral bioavailability properties (Bello *et al.,* 2025). The assessment was conducted using the SwissADME web tool, following the approaches outlined by Bello *et al.,* (2025) and Abdul-Hammed *et al.*, (2021). The bioavailability RADAR plot (Figure 2) illustrates the optimal physicochemical space for six key parameters influencing oral bioavailability: Lipophilicity (LIPO), Molecular Size (SIZE), Polarity (POLAR), Solubility (INSOLU), Unsaturation (INSATU), and Flexibility (FLEX). The pink region in the RADAR represents the most favorable zone for each property (Abdul-Hammed *et al.,* 2021). The recommended thresholds for these parameters are as follows: Molecular weight (SIZE): ≤ 500 g/mol, Topological polar surface area (TPSA, POLAR): 20–130 Å², Octanol–water partition coefficient (XLOGP3, LIPO): −0.7 to 5.0, Solubility (ESOL Log S, INSOLU): ≤ 6.0, Fraction of sp³ carbons (Csp³, INSATU): ≥ 0.25, Rotatable bonds (FLEX): ≤ 10 (Bello *et al.,* 2025). Most prioritised compounds fell within the range for molecular weight, polarity, lipophilicity, solubility and flexibility. Exceptions were quercetin (TPSA 131.36 Å², marginally above the limit), 1-O-feruloyl-β-D-glucose (TPSA 145.91 Å²) and cyclopentadecanone (TPSA 17.07 Å², below the lower limit). Daucosterol was the clearest outlier: its molecular weight (576.85 g/mol), XLOGP3 (7.74) and ESOL log S (−7.7) all fall outside the favourable range, indicating poor predicted solubility. The flavonoids and phenolic acids (quercetin, isorhamnetin, taxifolin, 2,3-dihydroflavon-3-ol, caffeic acid, vanillic acid) also fell below the Csp³ guideline (0–0.13), which is typical of planar aromatic compounds. Quercetin, taxifolin and caffeic acid each carried one PAINS alert, meaning they may show non-specific activity in assays, which should be considered when planning experiments.

Bioavailability scores were 0.55 for most compounds (0.56 for caffeic acid and 0.85 for vanillic acid), matching miglitol (0.55) and well above acarbose (0.17). Because acarbose acts locally in the gut lumen and is poorly absorbed by design, low systemic absorption is not necessarily a disadvantage for inhibitors of digestive enzymes, so these predictions mainly indicate how the compounds are likely to behave if systemic exposure is desired.

Table 7: Oral Bioavailability And Physicochemical Properties Of Selected *Allium Cepa* Phytochemicals And Standard Drugs

Ligand	Formula	Mass (g/mol)	TPSA (Å²)	Rotatable bonds	XLOGP3	WLOGP	ESOL Log S	Lipinski violations	Bioavailability score	PAINS alerts	Fraction Csp³	Synthetic accessibility
Daucosterol	C35H60O6	576.85	99.38	9	7.74	5.85	-7.7	1	0.55	0	0.94	8.02
Quercetin	C15H10O7	302.40	131.36	1	1.54	1.99	-3.16	0	0.55	1	0	3.23
2,3-Dihydroflavon-3-ol	C15H12O3	240.25	46.53	1	1.94	2.04	-2.98	0	0.55	0	0.13	3.20
Taxifolin	C15H12O7	304.25	127.45	1	0.95	0.86	-2.66	0	0.55	1	0.13	3.51
Isorhamnetin	C16H12O7	316.26	120.36	2	1.87	2.29	-3.36	0	0.55	0	0.06	3.26
1-O-Feruloyl-β-D-glucose	C16H20O9	356.32	145.91	6	-0.31	-1.35	-1.64	0	0.55	0	0.44	4.55
Diallyl sulfide	C6H10S	114.21	25.30	4	2.16	2.09	-1.64	0	0.55	0	0.33	2.34
Cyclopentadecanone	C15H28O	224.38	17.07	0	5.81	5.03	-4.89	0	0.55	0	0.93	2.53
Caffeic acid	C9H8O4	180.16	77.76	2	1.15	1.09	-1.89	0	0.56	1	0	1.81
Vanillic acid	C8H8O4	168.15	66.76	2	1.43	1.10	-2.02	0	0.85	0	0.12	1.42
Acarbose (standard)	C25H43NO18	645.60	329.01	13	-8.82	-8.72	2.57	3	0.17	0	0.88	7.25
Miglitol (standard)	C8H17NO5	207.22	91.49	2	-1.27	-1.24	0.29	0	0.55	0	0.50	3.02

TPSA, topological polar surface area; ESOL Log S, estimated aqueous solubility; PAINS, pan-assay interference compounds; Csp³, fraction of sp³-hybridized carbon atoms.

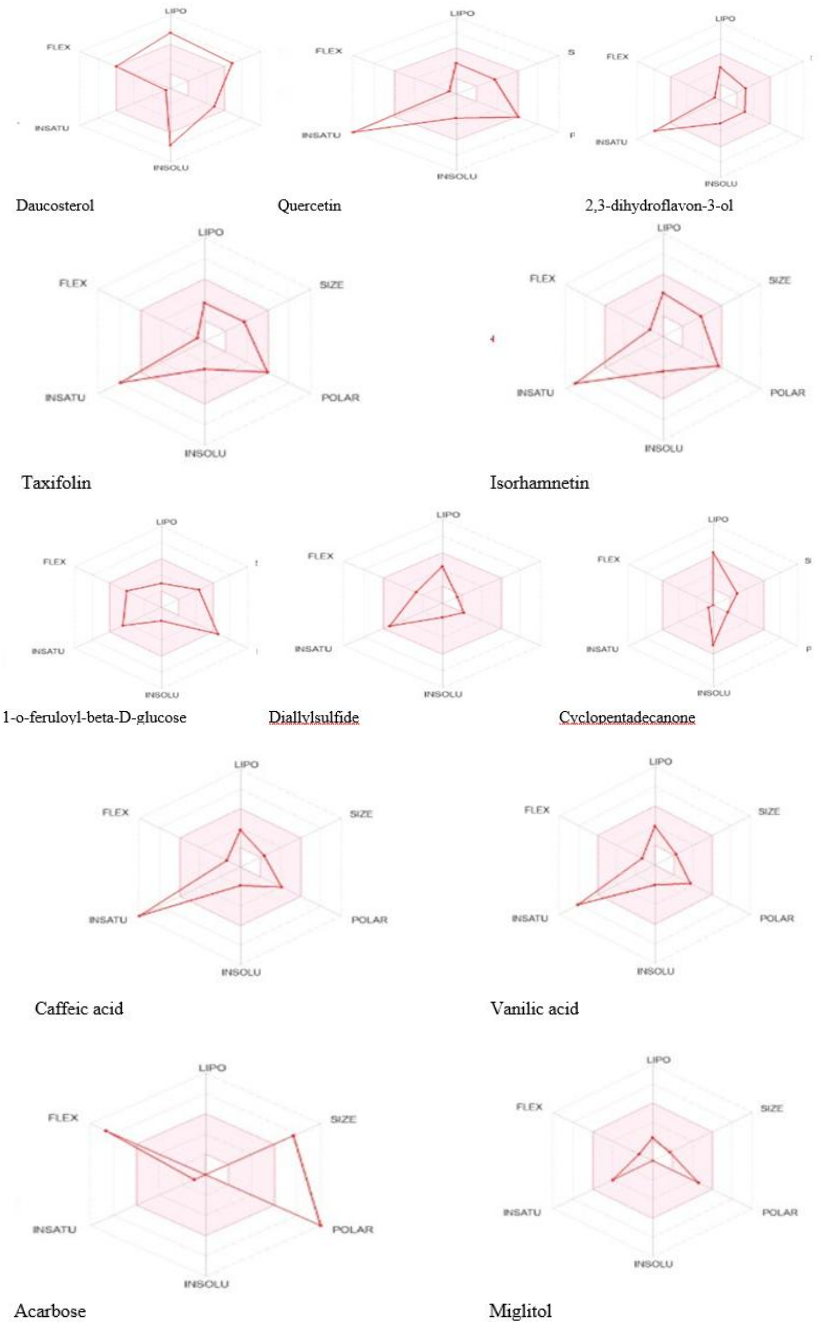


Figure 2: Bioavailability Radar of the Hit Compounds from *Allium Cepa* and Standard Drugs

PASS (Prediction of Activity Spectra for Substances) Analyses

Biological activity spectra were predicted with PASS, where Pa is the probability of activity and Pi the probability of inactivity (Table 8). Pa > 0.7 is considered high, 0.5–0.7 moderate and below 0.5 low (Filimonov *et al*., 2014). Most Pa values for the prioritised compounds were in the low-to-moderate range. 1-O-Feruloyl-β-D-glucose had a moderate predicted α-amylase inhibitor activity (Pa 0.595, Pi 0.003) and a moderate antidiabetic activity (Pa 0.511), and 2,3-dihydroflavon-3-ol had a moderate antidiabetic activity (Pa 0.513). Quercetin was predicted as an aldose reductase inhibitor (Pa 0.466) and α-glucosidase inhibitor (Pa 0.273), and daucosterol as antidiabetic (Pa 0.299) and α-glucosidase inhibitor (Pa 0.187). The predicted α-amylase inhibitor activity of daucosterol (Pa 0.124 against Pi 0.119) barely separates activity from inactivity and gives little support. For comparison, acarbose had high predicted α-glucosidase (Pa 0.987) and α-amylase (Pa 0.840) inhibitor activities. Overall, PASS offers limited support for the antidiabetic potential of these compounds, and the predictions are best viewed as hypotheses to test.

Table 8: Prediction Of Activity Spectra For The Selected Hit Compounds And Standards

Compounds	Biological Activity	Pa	Pi
Daucosterol	Antidiabetic	0.299	0.083
	Alpha-amylase inhibitor	0.124	0.119
	Alpha-glucosidase inhibitor	0.187	0.006
Quercetin	Antidiabetic (type 1)	0.195	0.019
	Aldose reductase inhibitor	0.466	0.003
	Alpha-glucosidase inhibitor	0.273	0.004
	Insulin sensitizer	0.100	0.047
2,3-Dihydroflavon-3-ol	Antidiabetic	0.513	0.021
	Alpha-amylase inhibitor	0.388	0.170
Taxifolin	Antidiabetic	0.462	0.029
Isorhamnetin	Aldose reductase inhibitor	0.437	0.003
1-O-Feruloyl-beta-D-glucose	Antidiabetic	0.511	0.022
	Alpha-amylase inhibitor	0.595	0.003
Cyclopentadecanone	Antidiabetic (type 1)	0.172	0.131
	Alpha-glucosidase inhibitor	0.119	0.019
Caffeic acid	Antidiabetic	0.385	0.048
	Aldose reductase inhibitor	0.160	0.008
	Alpha-glucosidase inhibitor	0.120	0.019
	Insulin sensitizer	0.153	0.024
Vanillic acid	Antidiabetic	0.252	0.112
	Insulin sensitizer	0.136	0.030
	Alpha-amylase inhibitor	0.463	0.009
Acarbose (Standard)	Alpha-glucosidase inhibitor	0.987	0.000
	Alpha-amylase inhibitor	0.840	0.001
	Antidiabetic	0.515	0.020
	Sodium/glucose cotransporter 2 inhibitor	0.045	0.004
Miglitol (Standard)	Alpha-amylase inhibitor	0.174	0.071
	Alpha-glucosidase inhibitor	0.725	0.010
	Antidiabetic	0.635	0.010
	Alpha-amylase inhibitor	0.486	0.007

Binding Mode and Molecular Interactions of the Hit Compounds and the Standards

i. Molecular interactions between ligands and the active sites of the target receptors are critical in rational drug design, as they provide valuable insights into the binding mechanisms that can guide lead optimization and improve affinity and selectivity (Abdul-Hammed *et al.,* 2021, Ikem *et al.,* 2026). As presented in Table 9 and Figure 3, the docking results revealed that the *Allium cepa* hit compounds interacted effectively with key residues of human pancrn eatic α-amylase, particularly within its catalytic pocket, through hydrogen bonding, lipophilic interactions, and electrostatic forces. Several ligands engaged residues essential for enzymatic catalysis and structural stability, including Asp197, Glu233, Asp300, Arg195, Asn298, Arg337, Asn100, Arg158, Asp167, and His201.

ii. Daucosterol formed hydrogen bonds with *Asp197* and *Glu233*, alongside electrostatic interactions with *Arg195*, *Asp197*, and *Glu233*. The interaction with *Arg195* is particularly noteworthy, as this residue coordinates the structural chloride ion vital for catalytic activity. Similarly, Quercetin established hydrogen bonds with *Glu233*, *Tyr62*, and *Gln63*, reinforcing its binding within the active site. 2,3-Dihydroflavon-3-ol exhibited both hydrogen and electrostatic interactions with *Gln63*, complemented by lipophilic contacts with *Tyr62* and *Trp59*, which contributed to binding stability.

iii. Taxifolin also demonstrated strong binding affinity through hydrogen bonds with *Asp300*, *His299*, and *Gln63*, along with electrostatic interactions involving *His299*, *Arg195*, and *Gln63*, as well as lipophilic interactions with *Arg195* and *Trp59*. While Cyclopentadecanone did not form hydrogen or electrostatic bonds, other ligands such as Isorhamnetin, Caffeic acid, Diallyl sulfide, and 1-O-feruloyl-beta-D-glucose exhibited strong hydrogen and electrostatic interactions with residues critical for maintaining the enzyme's active conformation.

iv. The standard drugs (Acarbose and Miglitol) displayed similar interaction patterns, engaging residues such as *Asp197*, *Glu233*, *Asp300*, *Arg195*, *Arg337*, *Arg158*, and *His201* through hydrogen bonding, electrostatic, and hydrophobic forces. The observed overlap in binding pockets between the standards and the hit compounds validates the hypothesis that these ligands occupy adjacent or overlapping catalytic regions known to be essential for enzymatic inhibition. Hence, these *Allium cepa* compounds may serve as promising scaffolds for further lead optimization, molecular dynamics simulations, and preclinical development toward novel antidiabetic agents.

v. Similarly, the docking analysis of *Allium cepa* compounds against human lysosomal acid α-glucosidase (GAA) (PDB ID: 5NN4) (Table 10 and figure 4) revealed strong interactions within the enzyme's active site. Key interacting residues included Arg89, Phe90, Asp91, Ala93, Pro94, Asp95, Lys96, Ala97, Ile98, Tyr110, Gly123, Gln124, Pro125, Trp126, Cys127, Trp273, Thr274, Arg275, and Asp319, which play major

roles in enzyme stability, substrate binding, and catalytic activity.

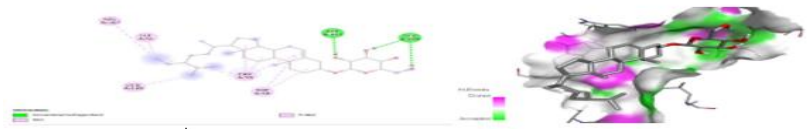
vi. Daucosterol formed hydrogen bonds with *Gly123*, electrostatic interactions with *Pro94* and *Gly123*, and lipophilic contacts with *Ala97*, *Trp126*, *Asp91*, *Pro125*, and *Trp273*. These interactions, particularly with *Ala97*, *Gly123*, *Pro125*, *Asp91*, and *Trp273*, located within the catalytic pocket, suggest potential inhibitory effects on the receptor's function. Quercetin also exhibited strong hydrogen bonding with *Pro94*, *Tyr543*, and *Arg331*, electrostatic interactions with *Tyr543*, *Arg275*, *Pro94*, and *Trp273*, and hydrophobic interactions with *Asp91* and *Ala93*, indicating possible receptor modulation.

vii. 2,3-Dihydroflavon-3-ol showed electrostatic interactions with *Arg594* and hydrophobic contacts with *Leu868*, *Val867*, *Leu865*, and *Val588*. Isorhamnetin primarily interacted with *Ala93* and *Ile98* via hydrogen bonding, and displayed additional lipophilic interactions with *Gly123* and *Trp126*, reinforcing its potential as an inhibitor. Taxifolin formed hydrogen bonds with *Ala93*, electrostatic interactions with *Trp126*, *Cys127*, and *Lys96*, and hydrophobic interactions with *Trp126*, *Asp91*, and *Pro125*, suggesting conformational modulation of the active site. Valinic acid formed hydrogen bonds with *Thr258*, *Gly259*, *His263* and lipophilic interactions with *Ala261*.

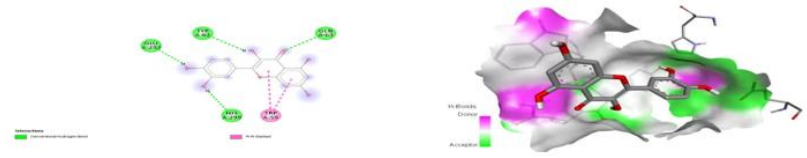
viii. The standard drugs (Acarbose and Miglitol) exhibited comparable interaction profiles, forming hydrogen, electrostatic, and hydrophobic interactions with *Ala93*, *Pro94*, *Lys96*, *Ile98*, *Gly123*, *Trp126*, *Cys127*, *His263*, *Ser265*, *Glu630*, and *Pro629*. Remarkably, these residues overlap with those engaged by the *Allium cepa* compounds, confirming their correspondence with the known active sites of the 5NN4 enzyme. Collectively, these findings predicted the potential of *Allium cepa* secondary metabolites as competitive inhibitors of α-amylase and α-glucosidase, suggesting their possible role in the development of novel antidiabetic therapeutics.

Table 9: Binding Mode, Molecular Interactions, And Electrostatic/Hydrophilic Interactions Of Hit Compounds And Standards With 1HNY

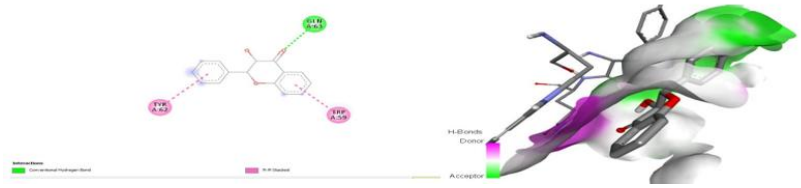
Compounds	Binding Affinity (ΔG), kcal/mol	Receptor Amino Acids Forming H-Bonds	Electrostatic or Hydrophilic Interactions	Lipophilic Interactions	Inhibition Constant (Ki), μM
Daucosterol	−9.7	ASP 197, GLU 233	ASP 197, ARG 195, GLU 233	VAL 107, ILE 51, LEU 165, TRP 59, TRP 58	0.08
Quercetin	−8.6	GLU 233	GLU 233, TYR 62, GLN 63, HIS 299	TRP 59, TYR 62, GLN 63, HIS 299	0.49
2,3-Dihydroflavon-3-ol	−8.5	GLN 63	GLN 63	TYR 62, TRP 59	0.58
Taxifolin	−8.5	ASP 300, HIS 299, GLN 63	HIS 299, ARG 195, GLN 63	ARG 195, TRP 59	0.58
Isorhamnetin	−8.1	GLU 233, GLN 63	GLU 233, ARG 195	TRP 59, ASP 300	1.15
1-O-Feruloyl-beta-D-glucose	−7.3	ASP 197, HIS 299, HIS 305, GLN 63	GLN 63, ASP 197, HIS 305	ASP 300, TRP 59, TYR 62	4.42
Cyclopentadecanone	−6.8	-	-	TRP 59	10.29
Caffeic acid	−6.4	GLN 63, HIS 299, ASP 300	HIS 299, ASP 300, GLU 233, GLN 63	ARG 195, ASP 197	20.2
Acarbose (Standard)	−6.5	GLU 240, LYS 200, GLU 233, ASP 197, GLN 63	LYS 200, GLU 233, HIS 101, GLN 63	TYR 151, TRP 59	17.08
Miglitol (Standard)	−5.5	HIS 101, ASP 300, TYR 62, ARG 195, GLU 233	GLU 233, ASP 300, HIS 299, HIS 101, ARG 195	ASP 197	92.48



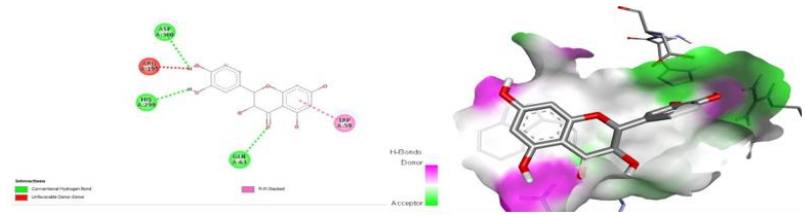
Daucosterol



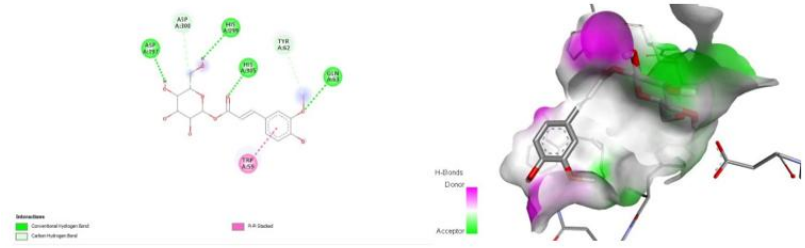
Quercetin



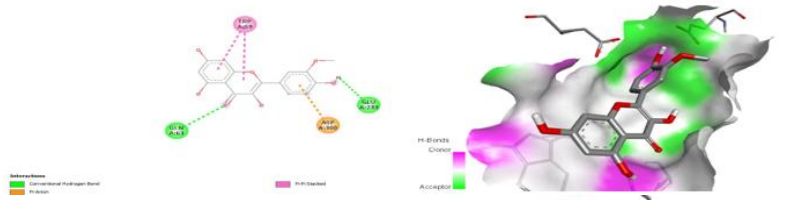
2,3-Dihydroflavon -3-ol



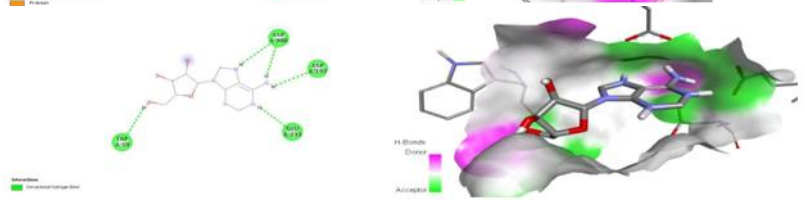
Taxifolin



Isorhamnetin



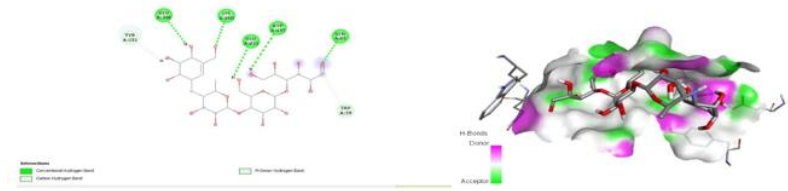
Diallyl sulfide



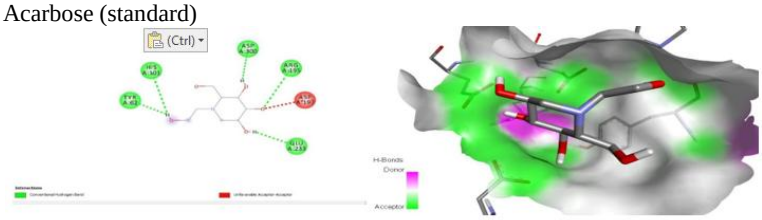
Cyclopentadecanone



Caffeic acid



Acarbose (standard)

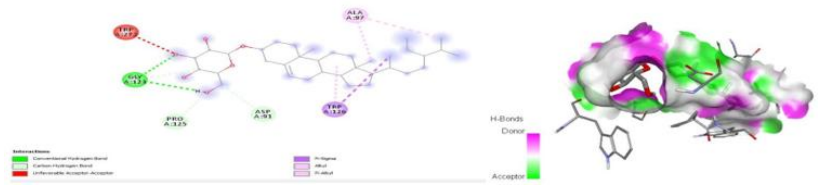


Miglitol (Standard)

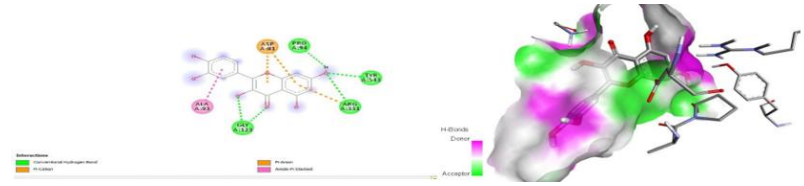
Fig 3: The Binding Mode and Molecular Interaction with 1HN

Table 10: Binding Affinities And Predicted Molecular Interactions Of Selected *Allium Cepa* Phytochemicals And Standard Drugs With Human Lysosomal Acid A-Glucosidase (PDB ID: 5NN4)

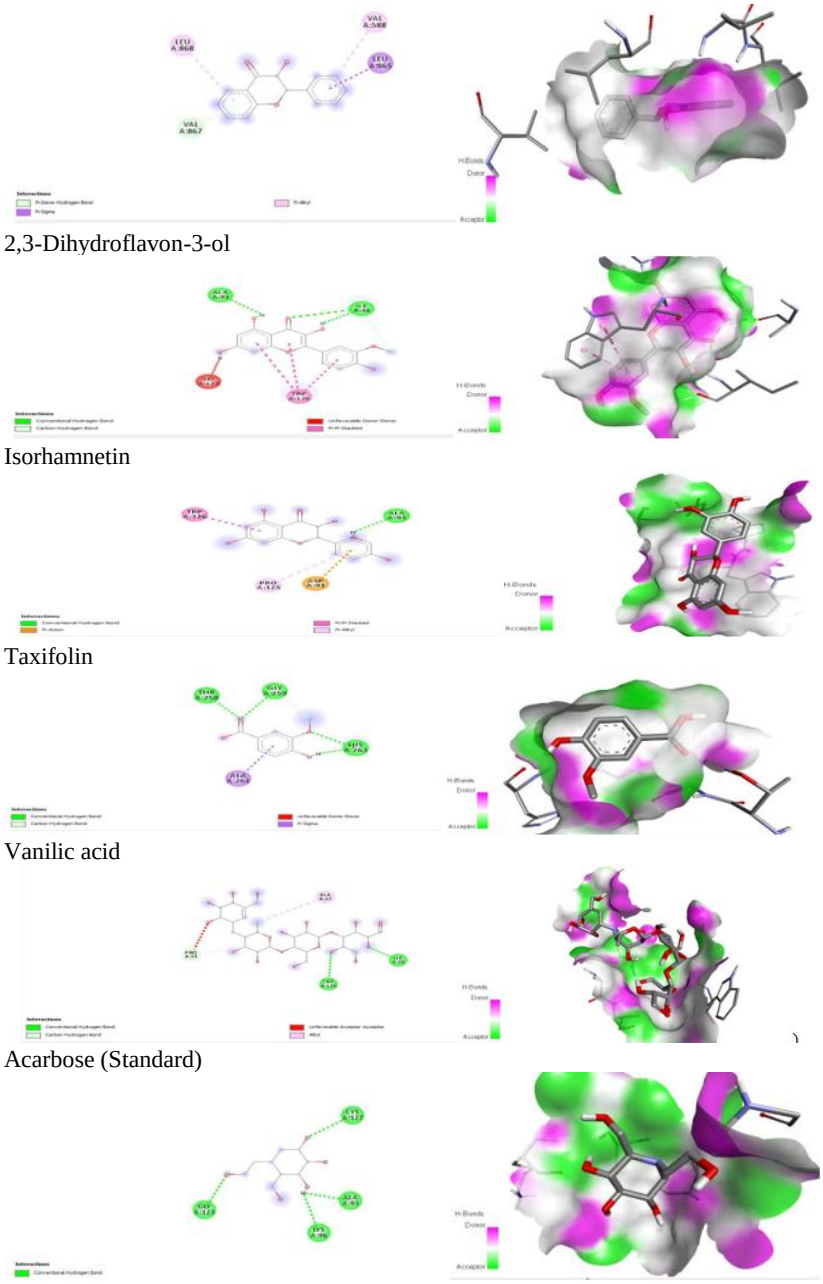
Compound	Binding Affinity, ΔG (kcal/mol)	Hydrogen-Bond Interactions	Electrostatic/Hydrophilic Interactions	Hydrophobic Interactions	Predicted Ki (μM)
Daucosterol	−8.2	GLY 123	PRO 94, GLY 123, ASP 91	ALA 97, TRP 126, PRO 125, TRP 273	0.97
Quercetin	−7.9	PRO 94, TYR 543	TYR 543, ARG 275, ARG 331, GLY 123	ASP 91, ALA 93, PRO 94, TRP 273	1.61
2,3-Dihydroflavon-3-ol	−7.4	Not reported	ARG 594	LEU 868, VAL 867, LEU 865, VAL 588	3.74
Isorhamnetin	−7.3	ALA 93, ILE 98	-	GLY 123, TRP 126	4.42
Taxifolin	−7.2	ALA 93	TRP 126, LYS 96, CYS 127	TRP 126, ASP 91, PRO 125	5.24
Vanillic acid	−6.9	THR 258, GLY 259, HIS 263	GLY 259, SER 265	ALA 261	8.69
Acarbose (Standard)	−6.9	TRP 126, ILE 98	CYS 127	ALA 97, PRO 94	8.69
Miglitol (Standard)	−5.1	GLY 123, CYS 127, ALA 93, LYS 96	PRO 94, GLY 123, LYS 96	-	181.72



Daucosterol



Quercetin



2,3-Dihydroflavon-3-ol

Isorhamnetin

Taxifolin

Vanilic acid

Acarbose (Standard)

Miglitol (Standard)

Fig 4: The Binding Mode and Molecular Interaction with Human Lysosomal Acid A-Glucosidase (PDB ID: 5NN4)

Discussion

Daucosterol and quercetin stand out for different reasons. Daucosterol (β-sitosterol glucoside) had the best docking score among the prioritised compounds against both enzymes. Its glucose moiety hydrogen-bonds with the catalytic residues of α-amylase, which is chemically plausible for a substrate-like sugar group. However, its large size (576.85 Da), high lipophilicity (XLOGP3 7.74) and poor predicted solubility (ESOL log S −7.7), together with a low ligand efficiency (0.24) and a high LELP (16.74), suggest that much of its docking score comes from size and hydrophobic contacts. Quercetin has a lower raw score but is far more efficient (LE 0.39), forms hydrogen bonds with Glu233, Tyr62, Gln63 and His299, and stacks on Trp59. Quercetin is also a flavonoid reported to inhibit these enzymes in vitro, and quercetin glucosides have recently been highlighted in onion peel studies (Drioiche *et al*., 2026), which adds plausibility. Its weaknesses are a PAINS alert, a TPSA just above the favourable limit, and predicted CYP1A2 and CYP3A4 inhibition.

Several limitations must be stated clearly. First, docking uses rigid receptors and an approximate scoring function, and Vina scores do not equal experimental binding energies. The scoring function favours large lipophilic molecules and handles polar sugar mimics such as acarbose poorly, so scoring better than acarbose does not mean stronger inhibition. This is also why terpenoids and saponins ranked highest, although many of them (for example the alliospirosides) failed Lipinski's rule and were not prioritised. Second, GAA was used as a structural surrogate. It is not the intestinal enzyme that controls glucose absorption, and inhibiting it is not a therapeutic goal, so the GAA results cannot be read as evidence of antidiabetic efficacy. Finally, no experimental data were generated.

CONCLUSION

This study screened 181 phytochemicals reported from *Allium cepa* against human pancreatic α-amylase and lysosomal acid α-glucosidase (GAA, used as a structural surrogate for the intestinal α-glucosidases) by molecular docking, followed by ADMET, drug-likeness, ligand-efficiency, oral bioavailability and PASS analyses. Daucosterol and quercetin emerged as the most interesting computational candidates. Daucosterol (−9.7 and −8.2 kcal/mol) and quercetin (−8.6 and −7.9 kcal/mol) scored better than acarbose (−6.5 and −6.9 kcal/mol) against α-amylase and GAA respectively, and both were predicted to bind near the catalytic residues of α-amylase. Quercetin showed better ligand efficiency and drug-likeness, whereas daucosterol is large, lipophilic and poorly soluble. The flavonoids 2,3-dihydroflavon-3-ol, taxifolin and isorhamnetin also showed favourable efficiency and drug-likeness. These results are predictions only: no enzyme-inhibition or toxicity experiments were performed, and docking scores are not experimental binding energies. Further investigations should prioritize molecular dynamics simulations to assess the stability of the predicted protein-ligand complexes, *in vitro* enzyme-inhibition assays to determine inhibitory activity against α-amylase and α-glucosidase, and appropriate kinetic studies to characterize the mode of inhibition of promising candidates. These experiments are essential to validate the computational predictions and establish whether the identified compounds have potential for further development as antidiabetic agents.

REFERENCES

Abdul-Hammed, M., Adedotun, I. O., Olajide, M., Irabor, C. O., Afolabi, T. I., Gbadebo, I. O., Rhyman, L., & Ramasami, P. (2021). *Virtual screening, ADMET profiling, PASS prediction, and bioactivity studies of potential inhibitory roles of alkaloids, phytosterols, and flavonoids against COVID-19 main protease (Mpro)*. *Natural Product Research*, 36(12), 3110-3116. https://doi.org/10.1080/14786419.2021.1935933

Adelusi, T. I., Oyedele, A.-Q. K., Boyenle, I. D., Ogunlana, A. T., Adeyemi, R. O., Ukachi, C. D., Idris, M. O., Olaoba, O. T., Adedotun, I. O., Kolawole, O. E., Xiaoxing, Y., & Abdul-Hammed, M. (2022). *Molecular modeling in drug discovery. Informatics in Medicine Unlocked*, *29*, 100880. https://doi.org/10.1016/j.imu.2022.100880

ADMETlab. (n.d.). Explanation of ADMET endpoints – ADMETlab 3.0. SCBDD. Retrieved September 26, 2025, from https://admetlab3.scbdd.com/explanation/

Ahmed, M. U., Ibrahim, A., Dahiru, N. J., & Mohammed, H. S. (2020). Alpha Amylase Inhibitory Potential and Mode of Inhibition of Oils from *Allium sativum* (Garlic) and *Allium cepa* (Onion). *Clinical Medicine Insights: Endocrinology and Diabetes*, *13*. https://doi.org/10.1177/1179551420963106

Bello I.A., Abdul-Hammed, M., John, A., Ismail, U., & Salis, M. (2025). *In silico* Analysis of Anti-asthmatic Potential of Phytochemicals from Moringa oleifera against S-nitrosoglutathione reductase and Interleukin-13. *International Journal of Chemistry and Chemical Processes E-ISSN*, *11*(1), 2025. https://doi.org/10.56201/ijccp.v11.no1.2025.pg19.56

Brayer, G. D., Luo, Y., & Withers, S. G. (1995). The structure of human pancreatic α-amylase at 1.8 Å resolution and comparisons with related enzymes. *Protein Science*, *4*(9), 1730–1742. https://doi.org/10.1002/pro.5560040908

Deshmukh, C. D., & Jain, A. (2015). Diabetes Mellitus: A Review. In *Int. J. Pure App. Biosci* (Vol. 3, Issue 3). www.ijpab.com

Durmaz, L., Kiziltas, H., Karagecili, H., Alwasel, S., & Gulcin, İ. (2023). Potential antioxidant, anticholinergic, antidiabetic and antiglaucoma activities and molecular docking of spiraeoside as a secondary metabolite of onion (*Allium cepa*). *Saudi Pharmaceutical Journal*, *31*(10). https://doi.org/10.1016/j.jsps.2023.101760

Falade, V. A., Adelusi, T. I., Adedotun, I. O., Abdul-Hammed, M., Lawal, T. A., and Agboluaje, S. A. (2021). *In silico* investigation of saponins and tannins as potential inhibitors of SARS-CoV-2 main protease (Mpro). *In silico* Pharmacology, 9(1), 1-15.

Fu, L., Shi, S., Yi, J., Wang, N., He, Y., Wu, Z., Peng, J., Deng, Y, Wang, W., Wu, C., Lyu, A., Zeng, X., Zhao, W., Hou, T., & Cao, D. (2024). ADMETlab 3.0: An updated comprehensive online ADMET prediction platform enhanced with broader coverage, improved performance, API functionality and decision support. Nucleic Acids Research, 52(W1), W422–W431. https://doi.org/10.1093/nar/gkae236

GBD 2021 Diabetes Collaborators. (2023). *Global, regional, and national burden of diabetes from 1990 to 2021, with projections of prevalence to 2050: A systematic analysis for the Global Burden of Disease Study 2021. The Lancet*, *402*(10397), 203–234. https://doi.org/10.1016/S0140-6736(23)01301-6

Halim, S. A., Lodhi, H. W., Waqas, M., Khalid, A., Abdalla, A. N., Khan, A., & Al-Harrasi, A. (2023). Targeting α-amylase enzyme through multi-fold structure-based virtual screening and molecular dynamic simulation. *Journal of Biomolecular Structure and Dynamics*, *41*(15), 5617–5630. https://doi.org/10.1080/07391102.2023.2227721

Hassan, S., Channar, P. A., Larik, F. A., Saeed, A., Shah, H. S., Lecka, J., Sévigny, J., & Iqbal, J. (2018). Synthesis of novel (E)-1-(2-(2-(4(dimethylamino) benzylidene) hydrazinyl)-4methylthiazol-5-yl)ethanone derivatives as ecto-50nucleotidase inhibitors. *Royal Society Open Science*, *5*(9). https://doi.org/10.1098/rsos.180837

Hedrington, M. S., & Davis, S. N. (2019). Considerations when using alpha-glucosidase inhibitors in the treatment of type 2 diabetes. *Expert Opinion on Pharmacotherapy*, *20*(18), 2229–2235. https://doi.org/10.1080/14656566.2019.1672660

Hossain, M. J., Al-Mamun, M., & Islam, M. R. (2024). Diabetes mellitus, the fastest growing global public health concern: Early detection should be focused. In *Health Science Reports* (Vol. 7, Issue 3). John Wiley and Sons Inc. https://doi.org/10.1002/hsr2.2004

Ibironke A., Abdul-Hammed, M., Bello, M., Ismail, U., & Oladepo, M. (n.d.). *Avocado Fruit Peel as a Source of Antidiabetic drugs: Evidence from Molecular Docking Studies and ADMET Profiling Article in INTERNATIONAL JOURNAL OF CHEMISTRY AND CHEMICAL PROCESSES · December 2024*. https://doi.org/10.56201/ijccp.v10.no6.2024.pg17.39

Ikem, D., Buzugbe, S., Okubor, P., & Michael, O. (2026). Comparative in silico ADMET Analysis of Berberine and Piperine: A rationale for combinatorial therapy to overcome p-glycoprotein-mediated efflux. *fudma journal of sciences*, 10(6), 16-20.

Lipinski, C.A. (2004). Lead profiling Lead-and drug-like compounds: the rule of five revolutions, Drug Discovery Today, 1(4):337-341

Manhas, D., Dhiman, S., Kour, H., Kour, D., Sharma, K., Wazir, P., Vij, B., Kumar, A., Sawant, S. D., Ahmed, Z., & Nandi, U. (2024). ADME/PK Insights of Crocetin: A Molecule Having an Unusual Chemical Structure with Druglike Features. *ACS Omega*, *9*(19), 21494–21509. https://doi.org/10.1021/acsomega.4c02116

Maulana, A. F., Sriwidodo, S., Rukayadi, Y., & Maksum, I. P. (2022). *In silico study of mangostin compounds and its derivatives as inhibitors of α-glucosidase enzymes for anti-diabetic studies. Biology*, *11*(12), 1837. https://doi.org/10.3390/biology11121837

Ogunyemi, B. T., Abdul-Hammed, M., Adedotun, I. O., Egunjobi, B. T., Badmos, S. T., Adegboyega, T. A., Aderogba, A. A., & Adeosun, G. G. (2025). Protein–ligand molecular dynamics simulation (PL-MDS), ADMET analyses, and bioactivity studies of phytochemicals from Aloe Vera: an In-Silico novel antidiabetics drug discovery effort. *Discover Chemistry*, *2*(1). https://doi.org/10.1007/s44371-025-00130-1

Roig-Zamboni, V., Cobucci-Ponzano, B., Iacono, R., Ferrara, M. C., Germany, S., Bourne, Y., Parenti, G., Moracci, M., & Sulzenbacher, G. (2017). Structure of human lysosomal acid α-glucosidase: A guide for the treatment of Pompe disease. *Nature Communications*, *8*, Article 1111. https://doi.org/10.1038/s41467-017-01263-3

Sharma, P., Joshi, T., Joshi, T., Chandra, S., & Tamta, S. (2020). *In silico* screening of potential antidiabetic phytochemicals from Phyllanthus emblica against therapeutic targets of type 2 diabetes. *Journal of Ethnopharmacology*, *248*. https://doi.org/10.1016/j.jep.2019.112268

Sim, L., Quezada-Calvillo, R., Sterchi, E. E., Nichols, B. L., & Rose, D. R. (2008). Human intestinal maltase–glucoamylase: Crystal structure of the N-terminal catalytic subunit and basis of inhibition and substrate specificity. *Journal of Molecular Biology*, *375*(3), 782–792.

Sim, L., Willemsma, C., Mohan, S., Naim, H. Y., Pinto, B. M., & Rose, D. R. (2010). Structural basis for substrate selectivity in human maltase-glucoamylase and sucrase-isomaltase N-terminal domains. *Journal of Biological Chemistry*, *285*(23), 17763–17770. https://doi.org/10.1074/jbc.M109.078980

Shoily, M. S. A., Islam, M. E., Rasel, N. M., Parvin, S., Barmon, J., Aqib, A. H., Roy, D. N., & Parvin, M. S. (2025). *Unveiling the biological activities of Heliotropium indicum L. plant extracts: Anti-inflammatory activities, GC–MS analysis, and in silico molecular docking. Scientific Reports*, *15*, 3285. https://doi.org/10.1038/s41598-024-79559-w

Sofian S. Mohamed, Salah M. Bensaber, Nisreen H. Meiqal, Anton Hermann, Abdul M. Gbaj, (2025), Design and In-Silico Evaluation of Pyridine-4-Carbohydrazide Derivatives for Potential Therapeutic Applications, J, Surgical Case Reports and Images, 8(3); DOI: https://doi.org/10.31579/26901897/235

Stoica, F., Aprodu, I., Enachi, E., Stănciuc, N., Condurache, N. N., Duță, D. E., Bahrim, G. E., & Râpeanu, G. (2021). Bioactive's characterization, biological activities, and *in silico* studies of red onion (*Allium cepa* L.) skin extracts. *Plants*, *10*(11). https://doi.org/10.3390/plants10112330

Sunday, A. O., Abdullahi, S., Gabriel, O. K., Moses, O., & Banjo, S. (2025). *In silico* Investigations of Triazole-Tromethoxyphenyl Derivatives as Anti-Proliferative Agents against Adenocarcinomic Human Alveolar Basal Epithelial Cells (A549): DFT, QSAR and Molecular Docking Approaches. *Kharkov University Bulletin Chemical Series*, *44*, 6–25. https://doi.org/10.26565/2220-637x-2025-44-01

Vivek-Ananth, R. P., Mohanraj, K., Sahoo, A. K., & Samal, A. (2023). *IMPPAT 2.0: An enhanced and expanded phytochemical atlas of Indian medicinal plants. ACS Omega*, *8*(8), 8827–8845. https://doi.org/10.1021/acsomega.3c00156

Zainab, B., Ayaz, Z., Alwahibi, M. S., Khan, S., Rizwana, H., Soliman, D. W., Alawaad, A., & Mehmood Abbasi, A. (2020). In-silico elucidation of Moringa oleifera phytochemicals against diabetes mellitus. *Saudi Journal of Biological Sciences*, *27*(9), 2299–2307. https://doi.org/10.1016/j.sjbs.2020.04.002

©2026 This is an Open Access article distributed under the terms of the Creative Commons Attribution 4.0 International license viewed via https://creativecommons.org/licenses/by/4.0/ which permits unrestricted use, distribution, and reproduction in any medium, provided the original work is cited appropriately.